Simulating the Air Quality Impact of Prescribed Fires Using a Graph Neural Network-Based PM$_{2.5}$ Emissions Forecasting System

Kyleen Liao
Saratoga High School
CA, USA
kyleenliao@gmail.com

Jatan Buch
Columbia University
NY, USA
jb4625@columbia.edu

Kara Lamb
Columbia University
NY, USA
kl3231@columbia.edu

Pierre Gentine
Columbia University
NY, USA
pg2328@columbia.edu

Abstract

The increasing size and severity of wildfires across western North America have generated dangerous levels of PM$_{2.5}$ pollution in recent years. In a warming climate, expanding the use of prescribed fires is widely considered to be the most robust fire mitigation strategy. However, reliably forecasting the potential air quality impact from these prescribed fires, a critical ingredient in determining the fires' location and time, at hourly to daily time scales remains a challenging problem. This paper proposes a novel integration of prescribed fire simulation with a spatio-temporal graph neural network-based PM$_{2.5}$ forecasting model. The experiments in this work focus on determining the optimal time for implementing prescribed fires in California as well as quantifying the potential air quality trade-offs involved in conducting more prescribed fires outside the fire season.

1 Introduction

Across many parts of the western United States (WUS), wildfire size, severity, and fire season length have increased due to climate change. Wildfires across the WUS have led to the largest daily mean PM$_{2.5}$ (particulate matter < 2.5 microns) concentrations observed by ground-based sensors in recent years (1), and exposure to PM$_{2.5}$ is responsible for 4.2 million premature deaths worldwide per year (2). Within California, additional PM$_{2.5}$ emissions from extreme wildfires over the past 8 years have reversed nearly two decades of decline in ambient PM$_{2.5}$ concentrations (3).

Prescribed fires, or controlled burns, have been widely accepted as an effective land management tool and could have the potential to reduce the resulting smoke from future wildfires (4). Since air quality is a major public concern surrounding prescribed fires (5), land managers conducting these burns require access to robust, near real-time predictions of downwind air pollution in order to determine suitable locations and burn windows.

This paper introduces a graph neural network (GNN) model that incorporates satellite observations of fire behavior in order to forecast PM$_{2.5}$ emissions from ambient sources, observed fires, and simulated controlled burns. Our GNN-based forecasting system can aid land managers in minimizing the PM$_{2.5}$ exposure of vulnerable populations during controlled burns and inform the public when proposing prescribed fires.

2   Related Work

Previous works studying the effect of prescribed fires used chemical transport models (CTMs) like the Community Multiscale Air Quality (CMAQ) and Goddard Earth Observing System Atmospheric Chemistry (GEOS-Chem) models to calculate the $PM_{2.5}$ impact of prescribed fires at different locations (4). While CTMs can model the chemical processes in $PM_{2.5}$ transport, generating accurate predictions requires a large volume of information because of the complex chemical interactions. Furthermore, the extensive calculations in CTMs make it challenging to explore a large range of parameters for simulating prescribed burns (6; 7; 8). In air quality predictions, machine learning models have been shown to outperform CTMs in terms of accuracy and computational burden (9). While several past works use machine learning to forecast air quality (10; 11), ours is the first research paper to our knowledge that utilizes machine learning to predict the $PM_{2.5}$ concentrations from simulated prescribed fires.

Our research builds upon the GNN machine learning model from Wang et al. (2020) (11), which was used to forecast non-wildfire-influenced $PM_{2.5}$ pollution in China. In contrast, this work focuses on simulating the effect of prescribed fires and predicting fire-influenced $PM_{2.5}$ in California.

3   Methods

3.1   Dataset

Our dataset consists of $PM_{2.5}$, meteorological, and fire data at an hourly resolution over 5 years (2017-2021). The $PM_{2.5}$ concentration data, at a total of 112 air quality sensor locations in California, is collected from both the California Air Resources Board as well as the Environmental Protection Agency (12; 13). The data for the 7 meteorological variables, which include u and v horizontal components of wind, total precipitation, and air temperature, are retrieved from the ERA5 Reanalysis database (14). The full list of predictors is in Table 1. Though the meteorological variables may capture the diurnal $PM_{2.5}$ cycles and seasonal patterns, the Julian date and hour of the day are also included as predictors in order to provide the model with additional context.

The fire radiative power (FRP) provides information about the fire intensity. The FRP at each fire location is taken from the Visible Infrared Imaging Radiometer Suite (VIIRS) (15) instrument on board the Suomi satellites. In order to assess the impact of nearby fires at the location of a $PM_{2.5}$ monitor, we aggregate the FRP values of all active fires within radii of 25km, 50km, 100km, and 500km. To emphasize the fires that would likely have a more substantial downwind effect on $PM_{2.5}$ concentrations, we use inverse distance weighting (IDW) and wind-based weighting in the FRP aggregation. This process is described in more detail in Appendix A. The number of fires within 500km of a $PM_{2.5}$ site is also included in the dataset. After compilation, the dataset's missing values were imputed using the MissForrest algorithm (16).

The prescribed fire data, retrieved from Cal Fire (17), is not represented as a variable in the training dataset, but instead used in Experiments 1 and 2 when simulating prescribed fires.

Table 1: GNN Predictors

Predictor Name	Unit	Source
Planetary Boundary Layer Height (PBLH)	m	ERA5 Reanalysis
u-component of wind	m/s	ERA5 Reanalysis
v-component of wind	m/s	ERA5 Reanalysis
2m Temperature	K	ERA5 Reanalysis
Dewpoint temperature	K	ERA5 Reanalysis
Surface pressure	Pa	ERA5 Reanalysis
Total precipitation	m	ERA5 Reanalysis
WIDW FRP within 25km, 50km, 100km, 500km	MW	VIIRS
Number of fires within 500km	1	VIIRS
Julian date	1	N/A
Time of day	1	N/A

Table 2: Training/Validation/Testing Split

Training	Validation	Testing
1/1/2017 - 12/31/2018	1/1/2020 - 12/31/2020	1/1/2021 - 12/31/2021

3.2 Graph Neural Network (GNN)

We trained a spatio-temporal graph neural network (GNN) model based on Wang et al. (2020) (11) to predict $PM_{2.5}$ concentrations at an hourly temporal resolution. The GNN model is integrated with a recurrent neural network (RNN) component, such that the model is able to capture both the spatial and temporal propagation of $PM_{2.5}$. The model's node features include the meteorological and fire-related variables, while the edge attributes include the wind direction and speed at the source node and the direction and distance between any two locations.

As shown in Table 2, for the GNN model, two years are used for training and one year each for validation and testing. The year 2019 is excluded during training, validation, and testing because the 2019 fire season was an outlier and was less damaging than the other years. Validating and testing the model on the years 2020 and 2021 respectively would help us gain a better understanding of the model's performance during intense fires. Our model produces forecasts for a prediction window of 48 hours into the future based on a historical window of 240 hours.

3.3 Prescribed Fire Simulations

The main contribution of this work is the novel simulation of the effect of prescribed fires in conjunction with the GNN-based prediction of the resulting $PM_{2.5}$ concentrations. This pipeline is illustrated in Figure 1. The prescribed fires are simulated by transposing historical controlled burns to target times, which are selected by matching the Cal Fire prescribed fire data with the VIIRS FRP data. The transposed prescribed fire FRP information is combined with the observed meteorological data at the target times and inputted into the GNN model, which produces the $PM_{2.5}$ predictions.

Using this pipeline, we perform two model experiments. Experiment 1 demonstrates how the GNN forecasting system can determine the optimal time to implement prescribed fires and focuses on the short-term pollution effect of prescribed fires. Experiment 2, on the other hand, focuses on quantifying the pollution impact of prescribed fires across months. In the rest of the section, we discuss each experiment in more detail:
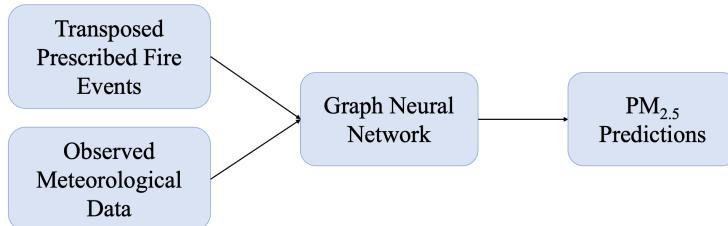

Figure 1: Prescribed Fire Simulation Pipeline

3.3.1 Experiment 1: Minimizing Prescribed Fire $PM_{2.5}$ Impact

To determine the optimal time to implement prescribed fires, we consider the immediate effect of prescribed fires. That is, we transpose the FRP values from actual prescribed fire events to target time points and add them to the observed FRP values at those points. As these FRP values are combined, they are aggregated using inverse distance and wind-based weighting, as outlined in Section 3.1 and Appendix A.

In this experiment, we transpose a window of time containing prescribed fires (1/3/21 - 1/15/21) to target times throughout the year 2021 at 24-hour time steps to simulate the air quality impacts of controlled burns. This window contains ten prescribed fires with burned areas above 100 acres.

Table 3: Results of the GNN, LSTM, and MLP Models

	GNN	LSTM	MLP
MAE	5.23	5.73	6.24
RMSE	6.72	7.32	7.83

Table 4: Results of PM$_{2.5}$ Predictions Based On Simulated Prescribed Fires

	Jan	Feb	Mar	Apr	May	Jun	Jul	Aug	Sep	Oct	Nov	Dec
Mean ($\mu g/m^3$)	15.62	15.64	14.69	15.18	14.76	15.92	18.44	21.73	18.55	16.95	19.94	18.73
Max ($\mu g/m^3$)	36.49	39.06	39.10	38.76	40.85	42.04	47.25	60.13	43.44	45.61	40.54	45.32

3.3.2 Experiment 2: Quantifying Prescribed Fire PM$_{2.5}$ Trade-Off

This experiment aims to quantify the pollution trade-off of implementing prescribed fires by simulating the effect of controlled burns in 2021 at the location of the Caldor fire. We employ two simulation techniques: one corresponding to the immediate effect of prescribed fires, and another related to simulating the longer-term effect of prescribed burning. For the former, we transpose historical prescribed fires near the location of the Caldor fire to the spring of 2021. In the latter case, we simulate the effect of controlled burns later in the year by excluding all FRP values within 25km of the Caldor fire between 8/14/21 and 10/21/21, implicitly assuming that a prescribed fire implemented earlier in the year (or even during the previous 1 to 2 fire seasons) could effectively mitigate a large fire in the same location a few months later. The PM$_{2.5}$ predictions from this counterfactual scenario are compared to baseline predictions derived using observed meteorological and fire inputs from 2021 without any prescribed fires around the Caldor fire locations. For more details, see Appendix B.

4 Results

The GNN model resulted in the lowest mean absolute error (MAE) and root mean squared error (RMSE) when compared with the long-short term memory (LSTM) and multilayer perception (MLP) models, as shown in Table 3. As a reference for the error, very unhealthy and hazardous PM$_{2.5}$ levels are ≥ 150.5 μg/m^3. Experiments 1 and 2 use the GNN and are the main focus of the results section.

4.1 Experiment 1: Minimizing Prescribed Fire PM$_{2.5}$ Impact

As shown in Table 4, the fall season, especially the month of August, was the least optimal time to implement prescribed fires since it resulted in the most significant PM$_{2.5}$ concentrations. As August is during the peak wildfire season, implementing prescribed fires would only exacerbate the already hazardous air quality. August's mean was 29.61% greater than the average mean of other months, and August's maximum was 44.27% greater than the average maximum of other months. The mean and maximum calculations are described in Appendix C. On the other hand, March, which had the lowest mean value, seemed to be an optimal month to implement prescribed fires.

4.2 Experiment 2: Quantifying Prescribed Fire PM$_{2.5}$ Trade-Off

The results support that, though prescribed fires may increase PM$_{2.5}$ in the short term, the prescribed fires reduce future PM$_{2.5}$ resulting from wildfires. As shown in Table 5, the simulated prescribed burns led the mean of the PM$_{2.5}$ predictions to be increased by an average of 0.31 μg/m^3 and the maximum PM$_{2.5}$ prediction to be increased by 3.07%. Details on the mean and maximum calculations are included in Appendix C. Table 5 also quantifies that the maximum of the predictions with the Caldor fire's influence removed was 52.85% lower than the maximum of the baseline predictions. Thus, the magnitude of the immediate PM$_{2.5}$ increase from the prescribed fire was significantly lower than the magnitude of the PM$_{2.5}$ decrease experienced during the fire season. Furthermore, excluding the influence of the Caldor Fire reduced the number of days with an unhealthy daily average PM$_{2.5}$ concentration from a mean of 3.54 days to 0.70 days. The reduction in PM$_{2.5}$ pollution after excluding the Caldor fire influence is illustrated in Figure 2, where the PM$_{2.5}$ monitoring sites are color-coded depending on the PM$_{2.5}$ pollution's US AQI level.

Table 5: Comparing the Predicted PM$_{2.5}$ Effect of Simulated Prescribed Burns With Baseline PM$_{2.5}$ Predictions

| | 3/21/21 - 5/31/21 | | 8/14/21 - 10/21/21 | |
	Simulated Prescribed Burn	Without Prescribed Burn (Baseline)	Removed Caldor Fire	With Caldor Fire (Baseline)
Mean ($\mu g/m^3$)	6.83	6.52	10.49	16.24
Max ($\mu g/m^3$)	55.78	54.12	83.61	177.32

(a) Removed Caldor Fire (b) With Caldor Fire (Baseline)
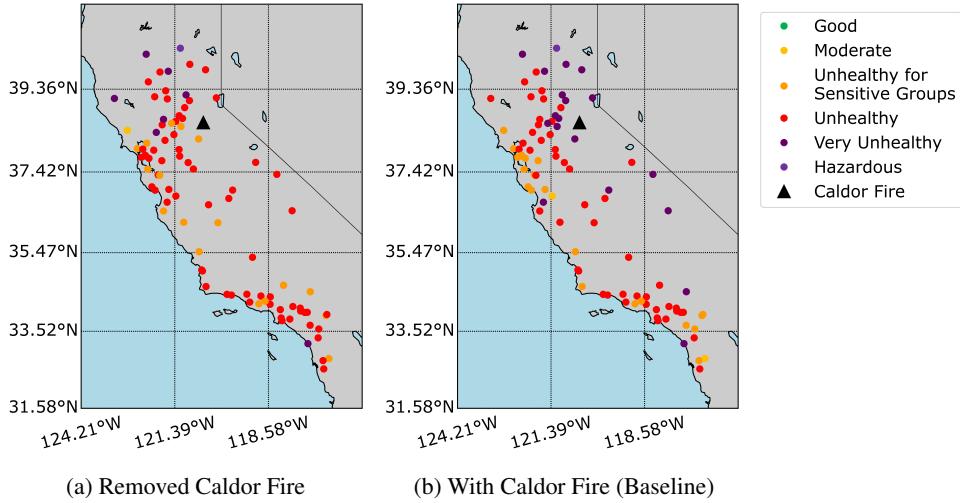
Figure 2: Maximum PM$_{2.5}$ predictions per site from 8/14/21 - 12/31/21 under condition (a) with prescribed burn at the Caldor Fire location during the spring and without Caldor Fire during the wildfire season and (b) without prescribed burn at the Caldor Fire location and with the Caldor Fire during the wildfire season

5 Conclusion and Future Work

To our knowledge, this is the first research paper to apply machine learning for simulating the PM$_{2.5}$ impact of prescribed fires, which is significant as machine learning is less computationally expensive than CTMs and requires lower expert curation of input variables. The primary contribution of this work is the prescribed fire simulation pipeline, which integrates prescribed fire simulations with GNN-based PM$_{2.5}$ predictions. Future work will focus on improving the fire simulation by incorporating physics-based modeling in the GNN framework. Our pipeline provides land managers and the fire service with a useful tool to minimize the PM$_{2.5}$ exposure of vulnerable populations, while also informing local communities of potential air quality impacts as well as beneficial trade-offs when implementing controlled burns.

6 Acknowledgements

References

[1] Burke, M., Driscoll, A., Heft-Neal, S., Xue, J., Burney, J., & Wara, M. (2021). The changing risk and burden of wildfire in the United States. *Proceedings of the National Academy of Sciences, 118*(2). https://doi.org/10.1073/pnas.2011048118

[2] World Health Organization. (2022). *Ambient (Outdoor) Air Pollution.* https://www.who.int/news-room/fact-sheets/detail/ambient-(outdoor)-air-quality-and-health

[3] Burke, M., Childs, M.L., de la Cuesta, B. et al. The contribution of wildfire to $PM_{2.5}$ trends in the USA. *Nature* (2023). https://doi.org/10.1038/s41586-023-06522-6

[4] Kelp, M. M., Carroll, M. C., Liu, T., Yantosca, R. M., Hockenberry, H. E., & Mickley, L. J. (2023). Prescribed Burns as a tool to mitigate future wildfire smoke exposure: Lessons for states and Rural Environmental Justice Communities. *Earth's Future, 11*(6).

[5] McCaffrey, Sarah M. 2006. Prescribed fire: What influences public approval . In: Dickinson, Matthew B., ed. 2006. Fire in eastern oak forests: delivering science to land managers, proceedings of a conference; 2005 November 15-17; Columbus, OH. Gen. Tech. Rep. NRS-P-1. Newtown Square, PA: U.S. Department of Agriculture, Forest Service, Northern Research Station: 192-198.

[6] Askariyeh, M. H., Khreis, H. & Vallamsundar, S. Air pollution monitoring and modeling. In Traffic-Related Air Pollut (eds Khreis, H. et al.) 111–135 (Elsevier, 2020).

[7] Byun, D. & Schere, K. L. Review of the governing equations, computational algorithms and other components of the models-3 community multiscale air quality (CMAQ) modeling system. *Appl. Mech. Rev* 59, 51–76 (2006).

[8] Zaini, N., Ean, L. W., Ahmed, A. N., Abdul Malek, M., & Chow, M. F. (2022). $PM_{2.5}$ forecasting for an urban area based on Deep Learning and Decomposition Method. *Scientific Reports, 12*(1). https://doi.org/10.1038/s41598-022-21769-1

[9] Rybarczyk, Y. & Zalakeviciute, R. Machine learning approaches for outdoor air quality modelling: A systematic review. *Appl. Sci.* https://doi.org/10.3390/app8122570 (2018).

[10] Li, L., Wang, J., Franklin, M. et al. Improving air quality assessment using physics-inspired deep graph learning. *npj Clim Atmos Sci* 6, 152 (2023). https://doi.org/10.1038/s41612-023-00475-3

[11] Wang, S., Li, Y., Zhang, J., Meng, Q., Meng, L., & Gao, F. (2020). $PM_{2.5}$-GNN. *Proceedings of the 28th International Conference on Advances in Geographic Information Systems.* https://doi.org/10.1145/3397536.3422208

[12] California Air Resources Board. Air Quality and Meteorological Information System [internet database] available via https://www.arb.ca.gov/aqmis2/aqmis2.php. Accessed June 7, 2023.

[13] US Environmental Protection Agency. Air Quality System Data Mart [internet database] available via https://www.epa.gov/outdoor-air-quality-data. Accessed June 7, 2023.

[14] Hersbach, H, Bell, B, Berrisford, P, et al. The ERA5 global reanalysis. *Q J R Meteorol Soc.* 2020; 146: 1999–2049. https://doi.org/10.1002/qj.3803

[15] Schroeder, W., Oliva, P., Giglio, L., & Csiszar, I. A. (2014). The new VIIRS 375 M active fire detection data product: Algorithm description and initial assessment. *Remote Sensing of Environment*, 143, 85–96. https://doi.org/10.1016/j.rse.2013.12.008

[16] Stekhoven, D. J., & Bühlmann, P. (2011). Missforest—non-parametric missing value imputation for mixed-type data. *Bioinformatics, 28*(1), 112–118. https://doi.org/10.1093/bioinformatics/btr597

[17] Cal Fire. Prescribed Burns [internet database] available via https://data.ca.gov/dataset/prescribed-burns. Accessed June 20, 2023.

[18] McClure, C. D., & Jaffe, D. A. (2018). US particulate matter air quality improves except in wildfire-prone areas. *Proceedings of the National Academy of Sciences, 115*(31), 7901–7906. https://doi.org/10.1073/pnas.1804353115
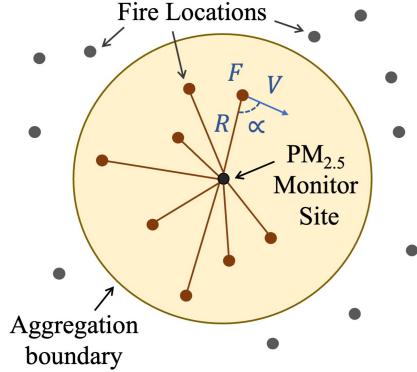
Figure 3: FRP Aggregation

A Fire Radiative Power (FRP) Aggregation

When creating the dataset, for each $PM_{2.5}$ monitor location, aggregations are performed on radii of 25km, 50km, 100km, and 500km to derive the wind and inverse-distance weighted (WIDW) FRP using the process described in Figure 3 and Equation 1,

$$F_{\text{WIDW}} = \sum_{i=1}^{n} \frac{F_i \, |V_i| \cos\left(|\alpha_i|\right)}{4\pi R_i{}^2} \tag{1}$$

where n is the number of fire locations within a certain radius of the $PM_{2.5}$ monitor site, F is the FRP value at the fire location, $|V|$ is the magnitude of the wind speed at the fire location, α is the relative angle between the wind direction and the direction from the fire to the $PM_{2.5}$ monitor, and R is the distance between the fire site and $PM_{2.5}$ monitor.

B Additional Details on Experiment 2 Methodology

This experiment simulates the effect of three prescribed fires, which were all within 20km of the 2021 Caldor fire, were active from 3/21 - 5/31 in 2018, 2019, and 2020 respectively, and burned around 6,300 acres each. Since the Caldor fire burned around 221,835 acres, we assume that preventing a fire of that scale would require a larger controlled burn. Thus, the FRP values from the prescribed fires are both artificially increased by a factor of 100 and transposed together to 2021, emulating a large prescribed fire from 3/21/21 to 5/31/21. As described in Section 3.3.1, the prescribed fires are transposed by combining the FRP values of the prescribed fires with the observed FRP values at the target time point, and then by aggregating those values using inverse distance weighting and the wind information at the target time points.

As mentioned in Section 3.3.2, for all time points after 5/31/21, the effect of prescribed burns later in the year are simulated by excluding all FRP values within 25km of the Caldor fire location. To further remove the Caldor fire influence, $PM_{2.5}$ values from 2018 are used as inputs instead of the Caldor-influenced, observed $PM_{2.5}$ values from 2021. The 2018 $PM_{2.5}$ data is chosen because, in comparison to the other years, the 2018 fire season most closely resembles the 2021 fire activity without fires at the Caldor fire location.

C Mean and Maximum Calculation Details

For Experiment 1, the mean and maximum values are calculated by averaging the mean and maximum $PM_{2.5}$ predictions of the locations whose $PM_{2.5}$ observations were $\geq 50 \ \mu g/m^3$ during the window 1/3/21 - 1/15/21. As the $PM_{2.5}$ observations at those locations are elevated during 1/3/21 - 1/15/21, they are likely influenced by the fire events that were transposed across the year 2021.

For Experiment 2, the mean and maximum values are calculated by averaging the mean and maximum $PM_{2.5}$ predictions of the 13 $PM_{2.5}$ monitor locations within 100km of the Caldor fire.